The Completed Probabilistic Modelling of Nanometer MIFGMOSFET

Rawid Banchuin[1] and **Roungsan Chaisricharoen**[2]

ABSTRACT

A completed model of the probabilistic distribution of the drain current's random variation of the nanometer multiple input floating gate MOSFET (MIFGMOSFET) is proposed in this work. The modelling process has taken the dominant physical level causes of the drain current's variations into account. Unlike its predecessor, the proposed model considers both N-type and P-type nanometer MIFGMOSFET. Moreover, the formerly neglected parasitic coupling capacitances have also been taken into account. The obtained modelling results, which are based on the derived drain current's equations of nanometer MIFGMOSFET, are very accurate. They can predict the probabilistic distributions of the candidate N-type and P-type nanometer MIFGMOSFETs obtained by using Monte-Carlo simulations with 99% confidence and higher accuracy than that of the previous work. We also perform a comparative robustness study of the nanometer MIFGMOSFET of both types and demonstrate various interesting applications of our modelling results.

Keywords: MIFGMOSFET, N-type, Nanometer, P-type, Probabilistic Modelling, Variability Aware Design

1. INTRODUCTION

The Floating gate MOSFET (FGMOSFET) has been adopted in many electronic circuits [1]-[11] where such devices at the nanometer level have also been applied. The efficiencies of these FGMOSFET based circuits can be deteriorated by the circuit level variations caused by the physical level nonidealities such as the random dopant fluctuation (RDF) and the line edge roughness (LER) etc. For both MOSFET and FGMOSFET, the key circuit level parameter is the drain current (I_D). The variations in other parameters can be obtained from the variation in I_D (ΔI_D). As a result, the modelling attempt of ΔI_D of MOSFET was derived in [12] where the nanometer level MOSFET was the focus. For the FGMOSFET, the analyses and modelling of variations in circuit level parameters have been previously performed using specific FGMOSFET based circuits [10], [11]. These previous results are not generic as they can be applied only to their dedicated circuits. Later, the probabilistic modelling of ΔI_D of a single FGMOSFET, which is therefore generic, was proposed in [13] and [14]. However, the results of these works are inapplicable to the FGMOSFET at nanometer regime because they have assumed above 100 nm CMOS technology. Recently, the probabilistic modelling of ΔI_D of the nanometer FGMOSFET has been proposed in [15] where the sub 100 nm CMOS technology and the FGMOSFET with multiple input namely MIFGMOSFET, have been assumed. Unfortunately, only the N-type device has been taken into account. There exists P-type nanometer MIFGMOSFET which employ different physical and device level characteristics including carrier type and noise immunity, thus a different probabilistic modelling is necessary. Moreover, the effects of the parasitic coupling capacitances, which are unavoidable in practice, have also been ignored.

Hence, the probabilistic modelling of ΔI_D of the nanometer MIFGMOSFET has been revisited in this work. Unlike [15], the formerly ignored P-type device and effects of the parasitic coupling capacitances have now been considered. The enhanced model's results are more detailed and complete. The aforementioned dominant physical level causes of the circuit level variations, such as RDF and LER, have been taken into account. The modelling results which are based on the parasitic coupling capacitances, including equations of I_D of nanometer MIFGMOSFET, have been found to be very accurate as they fit the probabilistic distributions of the candidate nanometer MIFGMOSFETs of both types obtained by using the 90 nm SPICE BSIM4 based Monte-Carlo simulation with a very high level of confidence (99%). Higher accuracy than that of [15] was achieved. We also perform the comparative studies of the robustness to physical level nonidealities of the nanometer MIFGMOSFET of both types. Moreover, we also demonstrate interesting applications of our modelling results such as the variability aware design involving nanometer MIFGMOSFET.

In the subsequent section, an overview of MIFGMOSFET will be given. The equations for I_D of nanometer MIFGMOSFET will be derived in section

Manuscript received on February 23, 2019; revised on March 29, 2020.
Final manuscript received on April 13, 2020.
[1] The author is with Graduated School of IT and Faculty of Engineering, Siam University, Bangkok, Thailand., E-mail: rawid_b@yahoo.com
[2] The author is with School of IT, Mae Fah Luang University, Chiangrai, Thailand., E-mail: roungsan.cha@mfu.ac.th
DOI: 10.37936/ecti-cit.2020142.123097

3. The proposed modelling is described in section 4. The verifications of the modelling results are presented in section 5. Applications are presented in section 6. Finally, the conclusion will be drawn in section 7.

2. THE OVERVIEW OF MIFGMOSFET

The MIFGMOSFET is a special MOSFET with multiple inputs and an additional gate isolated within the oxide entitled the floating gate. A cross sectional view, a symbolic diagram, and an equivalent circuit with parasitic coupling capacitances of an N-type with N inputs MIFGMOSFET can be depicted as in Fig. 1-3. The parasitic coupling capacitances was not assumed in [13]-[15]. C_{fb}, C_{fd} and C_{fs} denote the parasitic coupling capacitance between floating gate and substrate, the parasitic coupling capacitance between floating-gate and drain terminal, and the parasitic coupling capacitance between floating-gate and source terminal respectively. C_i and V_i denotes the input coupling capacitance between any ith input and the floating gate and the voltage at any ith input where $\{i\} = \{1, 2, 3, \ldots, N\}$.

From C_i's, C_{fb}, C_{fd} and C_{fs}, the coupling ratio of any ith input (k_i) can be defined as given by (1) which is unlike the previous definition [15]. This is because C_{fb}, C_{fd} and C_{fs} have been taken into account.

$$k_i = \frac{C_i}{\sum_{i=1}^{N}[C_i] + C_{fb} + C_{fd} + C_{fs}} \quad (1)$$

Similarly to k_i, we can define the coupling ratio of the bulk (k_{fb}), the drain terminal (k_{fd}) and the source terminal (k_{fs}) as follows:

$$k_{fb} = \frac{C_{fb}}{\sum_{i=1}^{N}[C_i] + C_{fb} + C_{fd} + C_{fs}} \quad (2)$$

$$k_{fd} = \frac{C_{fd}}{\sum_{i=1}^{N}[C_i] + C_{fb} + C_{fd} + C_{fs}} \quad (3)$$

$$k_{fs} = \frac{C_{fs}}{\sum_{i=1}^{N}[C_i] + C_{fb} + C_{fd} + C_{fs}} \quad (4)$$

3. THE PARASITIC COUPLING CAPACITANCES INCLUDED DRAIN CURRENT EQUATIONS OF NANOMETER MIFGMOSFET

Based on the coupling ratios given by (2)-(4) and the α-power law model [12][16], the equations of ID with parasitic coupling capacitances for the nanometer MIFGMOSFET can be derived by simply replacing the gate to source voltage term, V_{GS}, with $\sum_{i=1}^{N} k_i V_i + k_{fd}V_D + k_{fs}V_S + k_{fb}V_B - V_S$, where V_B, V_D and V_S stand for the body, drain, and source terminal voltages of the MIFGMOSFET. Therefore I_D of the nanometer MIFGMOSFET operated in triode and the saturation region can be respectively given by:

$$I_D = \beta\left[\frac{V_{DS}}{V_{DS,sat}} - \frac{1}{2}\left(\frac{V_{DS}}{V_{DS,sat}}\right)^2\right](\sum_{i=1}^{N} k_i V_i + k_{fd}V_D + k_{fs}V_S + k_{fb}V_B - V_S - V_t)^{\alpha} \quad (5)$$

$$I_D = \frac{\beta}{2}(\sum_{i=1}^{N} k_i V_i + k_{fd}V_D + k_{fs}V_S + k_{fb}V_B - V_S - V_t)^{\alpha} \quad (6)$$

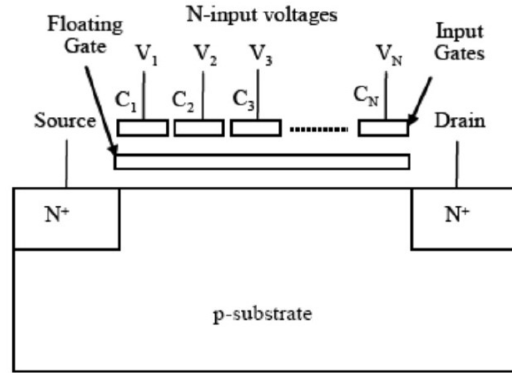

Fig.1: A cross sectional view of MIFGMOSFET [13]-[15].

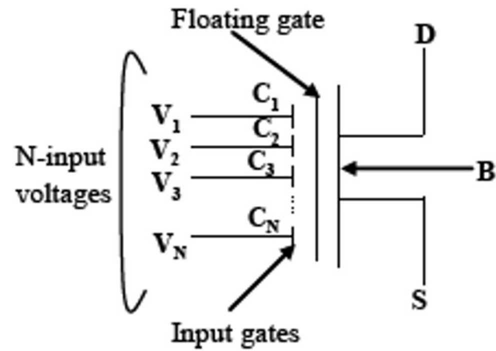

Fig.2: A symbolic diagram of MIFGMOSFET [13]-[15].

where V_t, β and V_{DS} stand for the threshold voltage, the current factor and the voltage dropped across drain and source terminals respectively. Moreover, $V_{DS,sat}$ and α denote V_{DS} at saturation and velocity saturation index where $1 \leq \alpha < 2$ [15]. These equations of I_D are more detailed than those of [15] because the effects of C_{fb}, C_{fd} and C_{fs} have been taken into account.

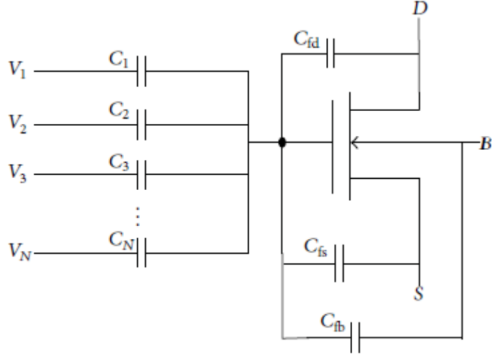

Fig.3: *An equivalent circuit model of MIFGMOSFET.*

Obviously, I_D is unintentionally altered by physical level nonidealities. Therefore the operating efficiency of FGMOSFET is deteriorated as mentioned above because such nonidealities alter the parameters of I_D. In particular, the RDF causes the variation V_t and the LER causes the variation in the channel length, which in turn causes the variation in β. As a result, the unwanted variation in I_D occurs and the operating efficiency of FGMOSFET is deteriorated. For illustration, I_D of a dual input N-type saturation region operated FGMOSFET has been simulated against V_1 assuming $V_2 = 0 = 0$ V as depicted in Fig. 4 and 5 which show that ±5% variations in V_t and β (which are respectively caused by RDF and LER) cause the variation in I_D.

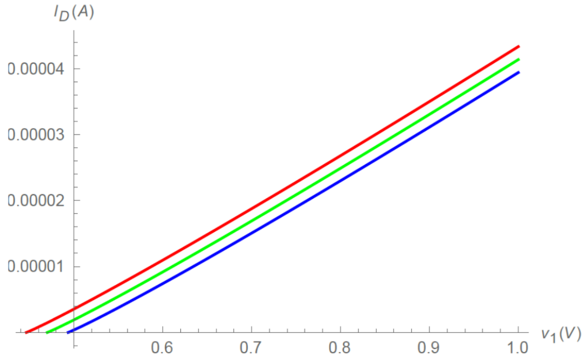

Fig.4: *The I_D of FGMOSFET with variation in V_t which is causes by RDF: -5% variation (red), no variation (green), +5% variation (blue).*

4. THE PROPOSED MODELLING

Similarly to [13]-[15], the proposed model has been derived as the probability density function of the normalized ΔI_D. A normalized ΔI_D i.e. $\Delta I_D/I_D$, can be defined with equation 7.

$$\frac{\Delta I_D}{I_D} = \frac{I_{Df} - I_D}{I_D} \tag{7}$$

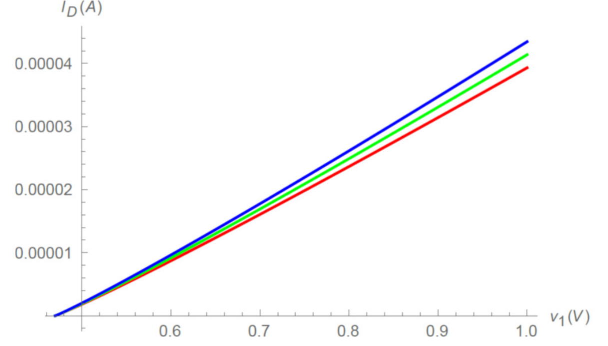

Fig.5: *The I_D of FGMOSFET with variation in β which is causes by LER: -5% variation (red), no variation (green), +5% variation (blue).*

I_{Df} denotes the fluctuated drain current which occurs when the physical level nonidealities have been taken into account. In this context, I_D stands for the ideal drain current where such nonidealities have been neglected [15]. On one hand, $\Delta I_D/I_D$ of the N-type nanometer MIFGMOSFET denoted by $\Delta I_{DN}/I_{DN}$ can be analytically given in terms of its physical level and device level parameters by equation 8.

$$\frac{\Delta I_{DN}}{I_{DN}} = \frac{\alpha[2\phi_F + C_{ox}^{-1}\sqrt{2qN_a(2\phi_F + V_S - V_B)\varepsilon_s} - (V_t - V_{FB})]}{\sum_{i=1}^{N} k_i V_i + k_{fd}V_D + k_{fs}V_S + k_{fb}V_B - V_S} \tag{8}$$

N_a, V_{FB}, V_B, ε_s and ϕ_F denote accepter doping concentration, flat band voltage, body voltage, dielectric constant of Si, and Fermi potential respectively [15]. Similarly to the equation of $\Delta I_D/I_D$ proposed in [15], (8) can describe $\Delta I_D/I_D$ of both triode and saturation region operated N-type nanometer MIFGMOSFETs, but in a more detailed manner. This is because k_{fb}, k_{fd} and k_{fs} have been included.

On the other hand, $\Delta I_D/I_D$ of the P-type nanometer MIFGMOSFET which has not been derived in [15], denoted by $\Delta I_{DP}/I_{DP}$, can be analytically given by equation 9.

$$\frac{\Delta I_{DN}}{I_{DN}} = \frac{\alpha[2|\phi_F| + C_{ox}^{-1}\sqrt{2qN_a(2|\phi_F| + V_S - V_B)\varepsilon_s} - (V_t - V_{FB})]}{V_S + V_t - \sum_{i=1}^{N} k_i V_i + k_{fd}V_D + k_{fs}V_S + k_{fb}V_B} \tag{9}$$

N_d denotes donor doping concentration. Similarly to (8), (9) can describe $\Delta I_D/I_D$ of both triode and saturation region operated P-type nanometer MIFGMOSFETs. At this point, it can be seen that the differences between N-type and P-type devices have been taken into account in the modelling process by using the different carrier related, N_a and N_d, the different polarities of V_B and V_S, and the different Fermi potential terms ϕ_F and $|\phi_F|$, in (8) and (9).

Based on the often cited and up-to-date Takeuchi's

model of the variation in scaled CMOS devices [17], the probability density functions of $\Delta I_{DN}/I_{DN}$ and $\Delta I_{DP}/I_{DP}$, $f_N(\delta I_{DN}/I_{DN})$ and $f_P(\delta I_{DP}/I_{DP})$, which are our modelling results, can be respectively given by equation 10 and 11.

$$f_N(\frac{\delta I_{DN}}{I_{DN}}) = \frac{\sum_{i=1}^{N} k_i V_i + k_{fd}V_D + k_{fs}V_S + k_{fb}V_B - V_S - V_t}{\alpha(2N_a(2\phi_F + V_S - V_B)\varepsilon_s)^{0.25}} \sqrt{\frac{3WLC_{ox}C_{inv}}{2\pi q^{1.5}}} \exp\left[-\frac{1.5WLC_{ox}C_{inv}(\sum_{i=1}^{N} k_i V_i + k_{fd}V_D + k_{fs}V_S + k_{fb}V_B - V_S - V_t)^2(\frac{\delta I_{DN}}{I_{DN}})^2}{(2N_a(2\phi_F + V_S - V_B)\varepsilon_s)^{0.5} q^{1.5}\alpha^2} \right] \quad (10)$$

$$f_N(\frac{\delta I_{DP}}{I_{DP}}) = \frac{\sum_{i=1}^{N} k_i V_i + k_{fd}V_D + k_{fs}V_S + k_{fb}V_B - V_S - V_t}{\alpha(2N_a(2\phi_F + V_S - V_B)\varepsilon_s)^{0.25}} \sqrt{\frac{3WLC_{ox}C_{inv}}{2\pi q^{1.5}}} \exp\left[-\frac{1.5WLC_{ox}C_{inv}(\sum_{i=1}^{N} k_i V_i + k_{fd}V_D + k_{fs}V_S + k_{fb}V_B - V_S - V_t)^2(\frac{\delta I_{DP}}{I_{DP}})^2}{(2N_a(2\phi_F + V_S - V_B)\varepsilon_s)^{0.5} q^{1.5}\alpha^2} \right] \quad (11)$$

W, L, $\delta I_{DN}/I_{DN}$, $\delta I_{DP}/I_{DP}$ and C_{inv} denote the channel width, the channel length, the sample variable version of $\Delta I_{DN}/I_{DN}$, that of $\Delta I_{DP}/I_{DP}$, and the inversion layer capacitance respectively. Of course, the derived $f_N(\delta I_{DN}/I_{DN})$ and $f_P(\delta I_{DP}/I_{DP})$ can be respectively applied to the N-type and P-type nanometer MIFGMOSFETs operating in both triode and saturation regions due to the operating region independent validities of the formulated $\Delta I_{DN}/I_{DN}$ and $\Delta I_{DP}/I_{DP}$.

5. THE ACCURACY VERIFICATION

Accuracy verification of $f_N(\delta I_{DN}/I_{DN})$ and $f_P(\delta I_{DP}/I_{DP})$ has been performed based on 90 nm level CMOS process technology with necessary parameters extracted by Predictive Technology Model (PTM). The nanometer dual input MIFGMOSFETs of both N-type and P-type with the input coupling ratios given by 0.617 and 0.283 for the 1st and 2nd input respectively have been chosen as our devices under test. These selected values of coupling ratios ensure that C_1 and C_2 are adequately large compared to C_{fb}, C_{fd} and C_{fs} in order to guarantee the proper operation of the candidate MIFGMOSFETs. It should be mentioned here that assuming adequately large Ci's has been performed in many previous works on MIFGMOSFET [6]-[8]. Since our candidate MIFGMOSFETs is a dual input device, we let $N = 2$ in both $f_N(\delta I_{DN}/I_{DN})$ and $f_P(\delta I_{DP}/I_{DP})$. We also assume $k_1 = 0.617$ and $k_2 = 0.283$. For the simulation with SPICE, such candidate MIFGMOSFETs have been modelled based on the MIFGMOSFET's equivalent circuit where the core nanometer MOSFETs of the devices have been modelled using BSIM4.

Similarly to [15], the convergence problem solving methodology presented in [18] has been adopted and $L = 90$ nm, $W/L = 4/3$, and $\alpha = 1.072$ have also been chosen. A supply voltage of 1.1 V has been assumed. Here, we also perform the verification in both qualitative and quantitative manners. In the qualitative aspect, $f_N(\delta I_{DN}/I_{DN})$ and $f_P(\delta I_{DP}/I_{DP})$ have been graphically compared to their benchmarks, $g_N(\delta I_{DN}/I_{DN})$ and $g_P(\delta I_{DP}/I_{DP})$, obtained from the Monte-Carlo simulation of the candidate devices. Also similarly to [15], 3000 runs have been chosen for the simulation because sufficiently detailed results with acceptable computational effort can be obtained. For the verification in the quantitative sense, the KolmogorovSmirnof goodness of fit test with confidence level of 99% has been performed based on the simulated data. See the appendix for details on the Kolmogorov-Smirnof test.

Since $f_N(\delta I_{DN}/I_{DN})$ and $f_P(\delta I_{DP}/I_{DP})$ are applicable to both triode and saturation region operated nanometer MIFGMOSFET of their respective types, their accuracies must be verified for both of these regions. In the qualitative aspect, $f_N(\delta I_{DN}/I_{DN})$ and $g_N(\delta I_{DN}/I_{DN})$ were graphically compared as respectively depicted in Fig. 6 and 7 for triode and saturation region operated nanometer N-type MIFGMOSFETs where $\Delta I_{DN}/I_{DN}$ which is dimensionless, has been expressed in percentage. Strong agreements between $f_N(\delta I_{DN}/I_{DN})$ and $g_N(\delta I_{DN}/I_{DN})$ were observed. In the quantitative aspect, the resulting test statistic for the triode device can be found as $KS = 0.01832$. For the saturation one, $KS = 0.01941$. Both of them are lower than the critical value given by $c = 0.0297596$. This means that $f_N(\delta I_{DN}/I_{DN})$ is accurate with 99% confidence for both regions of operation. Higher accuracy can be achieved for the triode region operated device. Moreover, it has been found that these KS values are lower than those of previous modelling results [11] of $KS = 0.024671$ and $KS = 0.026817$ for N-type triode and saturation region operated nanometer MIGMOSFETs respectively. Our result is more accurate. It should be mentioned here that the higher accuracy of our result is caused by the inclusion of C_{fb}, C_{fd} and C_{fs} in the modelling process.

For the P-type nanometer MIFGMOSFET on the other hand, the comparative plots of $f_P(\delta I_{DP}/I_{DP})$ and $g_P(\delta I_{DP}/I_{DP})$ were graphically compared as respectively depicted in Fig. 8 and 9 for triode and saturation region operated devices. Similarly to the qualitative verification of $f_N(\delta I_{DN}/I_{DN})$, the strong agreements between $f_P(\delta I_{DP}/I_{DP})$ and $g_P(\delta I_{DP}/I_{DP})$ were also observed. This qualitatively verifies the accuracy of $f_P(\delta I_{DP}/I_{DP})$. Moreover, the KS for the triode region device is $KS = 0.01866$. For the saturation one, it is $KS = 0.01891$. Both are lower than $c = 0.0297596$. Therefore $f_P(\delta I_{DP}/I_{DP})$ is accurate with 99% confidence for both regions of operation. Again, higher accuracy can also be achieved for the triode region operated device.

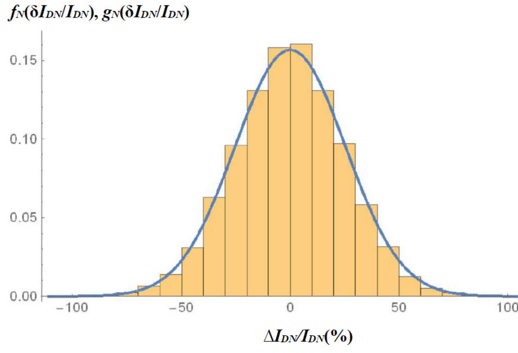

Fig.6: *The comparative plot of triode region based $f_N(\delta I_{DN}/I_{DN})$ (line) and $g_N(\delta I_{DN}/I_{DN})$ (histogram).*

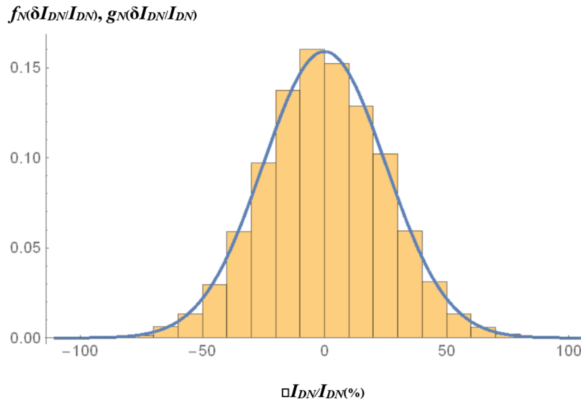

Fig.7: *The comparative plot of saturation region based $f_N(\delta I_{DN}/I_{DN})$ (line) and $g_N(\delta I_{DN}/I_{DN})$ (histogram).*

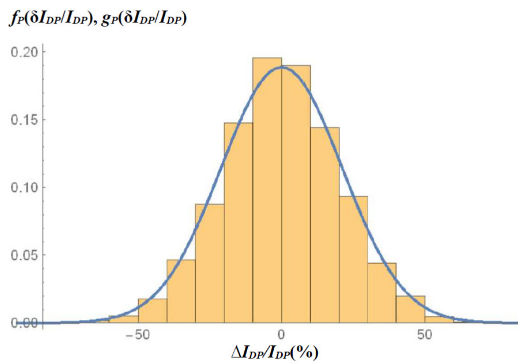

Fig.8: *The comparative plot of triode region based $f_P(\delta I_{DP}/I_{DP})$ (line) and $g_P(\delta I_{DP}/I_{DP})$ (histogram).*

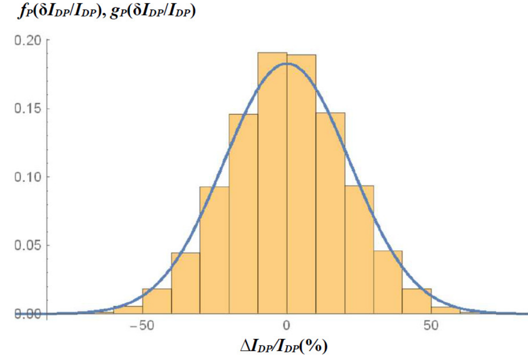

Fig.9: *The comparative plot of saturation region based $f_P(\delta I_{DP}/I_{DP})$ (line) and $g_P(\delta I_{DP}/I_{DP})$ (histogram).*

Before leaving this section, it should be mentioned here that the P-type nanometer MIFGMOSFET has been found to be more robust to the physical level nonidealities than its N-type counterpart for both triode and saturation regions. This is because $\Delta I_{DN}/I_{DN}$ is more widely distributed than $\Delta I_{DP}/I_{DP}$ as can be seen from Fig.4-7. Therefore the I_D of the N-type nanometer MIFGMOSFET suffers a more severe physical level nonidealities induced fluctuation. The physical reason behind this is a higher degree of RDF of N-type device which yields more variation in V_t.

6. THE APPLICATIONS OF THE MODELLING RESULTS

6.1 Analytical determination of the statistical parameters of drain current variations

By using $f_N(\delta I_{DN}/I_{DN})$ and $f_P(\delta I_{DP}/I_{DP})$, the statistical parameters of $\Delta I_{DN}/I_{DN}$ and $\Delta I_{DP}/I_{DP}$ can be analytically determined with the aid of the conventional statistical mathematics. Analytically obtaining these statistical parameters has been found to be beneficial to the nanometer MIFGMOSFET involved variability aware design as will be shown in the next subsection. It should be mentioned here that only the averages and variances of $\Delta I_{DN}/I_{DN}$ and $\Delta I_{DP}/I_{DP}$ will be treated in this section as the average and variance are the often cited statistical parameters. The derivations of other parameters, the probabilities related to $\Delta I_{DN}/I_{DN}$ and $\Delta I_{DP}/I_{DP}$ and some worthy of mentioned issues including the mathematical proof of certain existence of ΔI_D will be presented in the appendix.

The average of $\Delta I_{DN}/I_{DN}$ and that of $\Delta I_{DP}/I_{DP}$ can be mathematically defined by equation 12.

$$\overline{\frac{\Delta I_{Dj}}{I_{Dj}}} = \int_{-\infty}^{\infty} \frac{\delta I_{Dj}}{I_{Dj}} f_i\left(\frac{\delta I_{Dj}}{I_{Dj}}\right) d\left(\frac{\delta I_{Dj}}{I_{Dj}}\right) \tag{12}$$

j can be either N or P depending on the type of the

device under consideration.

After applying $f_N(\delta I_{DN}/I_{DN})$ and $f_P(\delta I_{DP}/I_{DP})$ to (12), we have $\overline{\frac{\Delta I_{DN}}{I_{DN}}} = \overline{\frac{\Delta I_{DP}}{I_{DP}}} = 0$.

On the other hand, the variances of $\Delta I_{DN}/I_{DN}$ and $\Delta I_{DP}/I_{DP}$, $\sigma^2_{\Delta I_{DN}/I_{DN}}$ and $\sigma^2_{\Delta I_{DP}/I_{DP}}$ can be mathematically defined by equation 13.

$$\sigma^2_{\frac{\Delta I_{Dj}}{I_{Dj}}} = \int_{-\infty}^{\infty} \left(\frac{\delta I_{Dj}}{I_{Dj}} - \overline{\frac{\Delta I_{Dj}}{I_{Dj}}} \right)^2 f_j(\frac{\delta I_{Dj}}{I_{Dj}}) d\frac{\delta I_{Dj}}{I_{Dj}} \tag{13}$$

By applying $f_N(\delta I_{DN}/I_{DN})$ and $f_P(\delta I_{DP}/I_{DP})$ to (17), we get equations 14 and 15.

$$\sigma^2_{\frac{\Delta I_{DN}}{I_{DN}}} = \frac{q^{1.5}\alpha^2\sqrt{2N_a(2\phi_F + V_S - V_B)\varepsilon_s}}{3WLC_{ox}C_{inv}(\sum_{i=1}^{N} k_iV_i + k_{fd}V_D + k_{fs}V_S + k_{fb}V_B - V_S - V_t)^2} \tag{14}$$

$$\sigma^2_{\frac{\Delta I_{DP}}{I_{DP}}} = \frac{q^{1.5}\alpha^2\sqrt{2N_a(2|\phi_F| - V_S + V_B)\varepsilon_s}}{3WLC_{ox}C_{inv}(\sum_{i=1}^{N} k_iV_i + k_{fd}V_D + k_{fs}V_S + k_{fb}V_B - V_S - V_t)^2} \tag{15}$$

It can be seen that $\sigma^2_{\Delta I_{DN}/I_{DN}} \neq 0$ and $\sigma^2_{\Delta I_{DP}/I_{DP}}$ $\neq 0$.

6.2 The nanometer MIFGMOSFET involved variability aware design

As promised, the usage of the statistical parameters and probabilities derived in the previous subsection in the variability aware design involving the nanometer MIFGMOSFET which refers to the applicability of $f_N(\delta I_{DN}/I_{DN})$ and $f_P(\delta I_{DP}/I_{DP})$ them self, will be demonstrated at this point. First of all, the minimization of ΔI_D which is an important part of such variability aware design, will be considered. From (14) and (15), we get equations 16 and 17.

$$\sigma^2_{\Delta I_{DN}/I_{DN}} \alpha \frac{1}{WL} \tag{16}$$

$$\sigma^2_{\Delta I_{DP}/I_{DP}} \alpha \frac{1}{WL} \tag{17}$$

Equations (16) and (17) state that lowering the device area of the nanometer MIFGMOSFET of any type causes an increasing in its ΔI_D as a penalty. The similar observation can also be obtained from the above 100 nm MIFGMOSFET [14]. Due to its penalty, such area lowering must be performed with caution. By using (14)-(17), we found equations 18 and 19.

$$WL \geq \frac{q^{1.5}\alpha^2\sqrt{2N_a(2\phi_F + V_S - V_B)\varepsilon_s}}{3C_{ox}C_{inv}(\sum_{i=1}^{N} k_iV_i + k_{fd}V_D + k_{fs}V_S + k_{fb}V_B - V_S - V_t)^2\sigma^2_{\Delta I_{DN}/I_{DN},\max}} \tag{18}$$

$$WL \geq \frac{q^{1.5}\alpha^2\sqrt{2N_a(2|\phi_F| - V_S + V_B)\varepsilon_s}}{3WLC_{ox}C_{inv}(\sum_{i=1}^{N} k_iV_i + k_{fd}V_D + k_{fs}V_S + k_{fb}V_B - V_S - V_t)^2\sigma^2_{\Delta I_{DP}/I_{DP},\max}} \tag{19}$$

$\sigma^2_{\Delta I_{Dj}/I_{Dj},\max}$ denotes the maximum acceptable value of $\sigma^2_{\Delta I_{Dj}/I_{Dj}}$. Both equations 18 and 19 must be satisfied for any variability aware design involving the nanometer MIFGMOSFET for ensuring an acceptable level of ΔI_D. Moreover, since $\sigma^2_{\Delta I_{Dj}/I_{Dj}}$ is directly related to the level of ΔI_D, the objective functions in equations 20 and 21 where 2 $\sigma^2_{\Delta I_{DN}/I_{DN}}$ and $\sigma^2_{\Delta I_{DP}/I_{DP}}$ serve as the basis, have been found to be useful.

$$\min[\sigma^2_{\Delta I_{DN}/I_{DN}}] \tag{20}$$

$$\min[\sigma^2_{\Delta I_{DP}/I_{DP}}] \tag{21}$$

Now the computationally efficient variability aware simulation of the nanometer MIFGMOSFET based circuit, which is also important to its variability aware design, will be considered. Since ΔI_D's of the MIFGMOSFETs within the circuit exhibit no spatial correlations [14], the variance of the random variation in the key parameter of any nanometer MIFGMOSFET based circuit (ΔX) i.e. $\sigma^2_{\Delta X}$, can be determined by using equation 22.

$$\sigma^2_{\Delta X} = \sum_{m=1}^{M} [\left(I_{Dm}S^X_{I_{Dm}}\right)^2 \sigma^2_{\frac{\Delta I_{Dm}}{I_{Dm}}}] \tag{22}$$

I_{Dm}, $S^X_{I_{Dm}}$ and $\sigma^2_{\Delta I_{Dm}/I_{Dm}}$ stands for the ideal drain current of an arbitrary m$^{\text{th}}$ nanometer MIFGMOSFET in the circuit, the sensitivity of the circuit's key parameter (X) with respect to I_{Dm}, which measures the amount of change in X with respected to the change in I_{Dm}, and the variance of the per-unit ΔI_{Dm} of any m$^{\text{th}}$ MIFGMOSFET. It should be mentioned here that there exist no correlation terms in (22) due to the lack of the special correlations as stated above.

By using either $\sigma^2_{\Delta I_{DN}/I_{DN}}$ or $\sigma^2_{\Delta I_{DP}/I_{DP}}$ depending on the type of such mth device, $\sigma^2_{\Delta I_{Dm}/I_{Dm}}$can be predetermined. After obtaining all $\sigma^2_{\Delta I_{DN}/I_{DN}}$'s, $\sigma^2_{\Delta X}$ can be numerically determined in a computationally effective manner by using (22) and a small signal analysis based simulation [14][19]. With such methodology, the whole set of $S^X_{I_{Dm}}$'s can be evaluated via the sensitivity analysis in which the circuit under consideration requires only one calculation for obtaining its solution [14] [20]. Therefore the consumed computational effort can be significantly reduced from that of the traditional Monte-Carlo simulation which may require hundreds or thousands of runs.

Apart from using the simulation, the amount of ΔX can also be analytically determined by us-

ing $\sigma^2_{\Delta I_{DN}/I_{DN}}$ and $\sigma^2_{\Delta I_{DP}/I_{DP}}$. This means that $f_N(\delta I_{DN}/I_{DN})$ and $f_P(\delta I_{DP}/I_{DP})$ can be applied to such analytical determination of ΔX, which is also an important part of the nanometer MIFGMOSFET involved variability aware design beside those aforementioned. In order to do so, the mathematical definition of $S^X_{I_{Dm}}$ defined according to the definition of sensitivity [21] as given by (23), which is different from the aforesaid meaning of $S^X_{I_{Dm}}$ assumed in the simulation for determining $\sigma^2_{\Delta X}$ stated above, must be adopted.

$$S^X_{I_{Dm}} = \frac{I_{Dm}}{X}\frac{\partial X}{\partial I_{Dm}} \tag{23}$$

For convenience, we will determine the amount of ΔX in terms of the variance of its per-unit value, $\sigma^2_{\Delta X/X}$. By using the above mathematical definition of $S^X_{I_{Dm}}$, we get equation 24

$$\sigma^2_{\frac{\Delta X}{X}} = \sum_{m=1}^{M}[\left(\frac{I_{Dm}}{X}\frac{\partial X}{\partial I_{Dm}}\right)^2 \sigma^2_{\frac{\Delta I_{Dm}}{I_{Dm}}}] \tag{24}$$

As an illustrative example, let X be the outward current (I_{out}) of the nanometer MIFGMOSFET based summing squarer [9] depicted in Fig. 10. By assuming that weighted sum of inputs is nonnegative, I_{out} can be given by [9] equation 25.

$$I_{out} = A_I I_{DN} + I_{DP} \tag{25}$$

A_I , I_{DN}, and I_{DP} are the gain of the current mirror, I_D of Q1, which is of N-type, and I_D of Q2, which is a P-type device respectively.

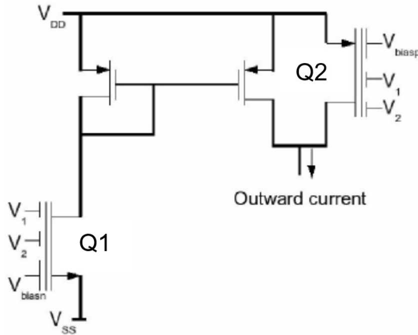

Fig.10: *The nanometer MIFGMOSFET based summing squarer [9].*

By using (25), we get equations 26 and 27.

$$\frac{\partial I_{out}}{\partial I_{DN}} = A_I \tag{26}$$

$$\frac{\partial I_{out}}{\partial I_{DP}} = 1 \tag{27}$$

As a result, $\sigma^2_{\Delta I_{out}/I_{out}}$ can be obtained in terms of $\sigma^2_{\Delta I_{DN}/I_{DN}}$ and $\sigma^2_{\Delta I_{DP}/I_{DP}}$ as seen in equations 28.

$$\sigma^2_{\frac{\Delta I_{out}}{I_{out}}} = \left(\frac{A_I I_{DN}}{A_I I_{DN} + I_{DP}}\right)^2 \sigma^2_{\frac{\Delta I_{DN}}{I_{DN}}} + \left(\frac{I_{DP}}{A_I I_{DN} + I_{DP}}\right)\sigma^2_{\frac{\Delta I_{DP}}{I_{DP}}} \tag{28}$$

I_{DN} and I_{DP} can be determined by using (6) with N = 3. This is because both Q1 and Q2 operate in the saturation region [9] and employ 3 inputs as can be seen from Fig. 10.

7. CONCLUSIONS

The probabilistic modelling of ΔI_D of nanometer MIFGMOSFET has been performed by taking the physical level nonidealities into consideration. Unlike [15], the formerly ignored P-type nanometer MIFGMOSFET and effects of C_{fb}, C_{fd} and C_{fs} have also been considered. The modelling results which are based on the derived equations of ID of nanometer MIFGMOSFET, can accurately predicts their benchmarks obtained from the 90 nm SPICE BSIM4 based Monte-Carlo simulation of the candidate devices with 99% confidence where higher accuracy than that of [15] can be achieved as can be seen from the lower KS of the results of this work. This accuracy improvement is caused by inclusion of C_{fb}, C_{fd} and C_{fs} in the modelling process. We have also found that the P-type nanometer MIFGMOSFET is more robust to the physical level nonidealities than its N-type counterpart for both triode and saturation regions of operation due to its lower degree of RDF.

Motivated by the thorough analysis of the above 100 nm device [14], many helpful statistical parameters and probabilities related to the nanometer MIFGMOSFET have been derived. In addition, the certain existence of ΔI_D of nanometer MIFGMOSFET has been mathematically proved. These interesting issues have been presented in the appendix. Moreover, the application of our results to the variability aware design involving the nanometer MIFGMOSFET have been pointed out. Therefore this work is highly beneficial to the analysis and design of any electronic circuit constructed based on the nanometer MIFGMOSFET.

ACKNOWLEDGEMENTS

The first author would like to acknowledge Mahidol University, Thailand, for the use of their online database service.

References

[1] S.K. Saha, "Design Considerations for Sub-90 nm Split-Gate Flash Memory Cells," *IEEE Transactions on Electron Devices*, Vol. 54, No. 11, pp. 3049–3055, 2007.

[2] S.K. Saha, "Scaling Considerations for Sub-90 nm Split-Gate Flash Memory Cells," *IET circuits, devices & systems*, Vol. 2, No. 1, pp. 144-150, 2008.

[3] S.K. Saha, "Non-linear Coupling Voltage of Split Gate Memory Cells with Additional Top Coupling Gate," *IET circuits, devices & systems*, Vol.6, No. 3, pp. 204-210, 2012

[4] C-W. Cao, S-G. Zang, X. Lin, Q-Q. Sun, C. Xing, P-F. Wang, and D. W. Zhang, "A Novel 1T-1D DRAM Cell for Embedded Application," *IEEE Transactions on Electron Devices*, Vol. 59, No. 5, pp. 1304-1310, 2012.

[5] D. Schinke, N. D. Spigna, M. Shiveshwarkar, and P. Franzon, "Computing with Novel Floating Gate Devices," *Computer*, Vol. 44, No. 2, pp. 29-36, 2011.

[6] R. Pandey and M. Gupta, "FGMOS based Voltage Controlled Grounded Resistor," *Radio Engineering*, Vol. 19, No. 3, pp. 455–459, 2010

[7] V. Suresh Babu, R.S. Devi, A. Sekhar amd M.R. Baiju, "FGMOSFET Circuit for Neuron Activation Function and Its Derivative," *Proceedings of the 4th IEEE conference on industrial electronics and applications (ICIEA09)*, pp. 739–744, 2009.

[8] E. Rodriguez-Villegas, A. Yufera and A. Rueda, "A 1.25-V Micropower Gm-C Filter Based on FG-MOS Transistors Operating in Weak Inversion," *IEEE Journal of Solid-State Circuits*, Vol. 39, No. 1, pp. 100–111, 2004

[9] B. Ramasubramanian, "A New Wide Input-range FGMOS Based Four Quadrant Multiplier with Electrical Error Correction," *Proceedings of the 2007 International Symposium on Signals, Circuits and Systems (ISCAS07)*, pp. 1-4, 2007

[10] S. Vlassis and S. Siskos, "Design of Voltage-mode and Current-mode Computational Circuits using Floating-Gate MOS Transistors," *IEEE Transactions on Circuits and Systems I: Regular Papers*, Vol. 51, No. 2, pp. 329-341, 2004.

[11] Y. Zhai and P. A. Abshire, "Adaptive Log Domain Filters for System Identification using Floating Gate Transistors," *Analog Integrated Circuits and Signal Processing*, Vol.56, No. 1-2, pp.23–36, 2008.

[12] K. Hasegawa, M. Aoki, T. Yamawaki, S. Tanaka, "Modeling Transistor Variation Using α-power Formula and Its Application to Sensitivity Analysis on Harmonic Distortion in Differential Amplifier," *Analog Integrated Circuits and Signal Processing*, Vol. 72, No. 3, pp 605–613, 2012.

[13] R. Banchuin and R. Chaisricharoen. "The Probabilistic Modeling of Random Variation in FG-MOSFET," *Proceedings of the 13th International Conference on Electrical Engineering/Electronics, Computer, Telecommunications and Information Technology (ECTI-CON)*, pp. 1-4, 2016.

[14] R. Banchuin and R. Chaisricharoen, "Probabilistic Modelling of Variation in FGMOSFET," *ECTI Transactions on Computer and Information Technology*, Vol. 11, No. 1, 50-62, 2017.

[15] R. Banchuin and R. Chaisricharoen, "Probabilistic Model of Nanometer MIFGMOSFET," *Proceedings of the 14th International Conference on Electrical Engineering/Electronics, Computer, Telecommunications and Information Technology (ECTI-CON)*, pp. 781-784, 2017.

[16] L. Bisdounis, "Short Circuit Energy Dissipation Model for Sub 100 nm CMOS Buffers," *Proceedings of the 17th IEEE International Conference on Electronics, Circuits, and Systems (ICECS)*, pp. 615-618, 2010.

[17] K. Takeuchi, A. Nishida and T. Hiramoto, "Random Fluctuations in Scaled MOS Devices," *Proceedings of the 2009 International Conference on Simulation of Semiconductor Processes and Devices (SISPAD09)*, pp. 79-85, 2009.

[18] J. Ramirez-Angulo, G. Gonzlrlez-Altamirano and S. C. Choi, "Modeling Multiple-input Floating-gate Transistors for Analog Signal Processing," *Proceedings of the 1997 International Symposium on Signals, Circuits and Systems (ISCAS97)*, pp. 2020-2023, 1997.

[19] A.H. Haddad, Probabilistic Systems and Random Signals, Prentice Hall, New Jersey, 2006.

[20] G. Cijan, T. Tuma and A. Burmen, "Modelling and Simulation of MOS Transistor Mismatch," *Proceeding of the 6th Eurosim Congress on Modeling and Simulation (EUROSIM 07)*, pp. 1-8, 2007.

[21] G. Daryanani, *Principle of Active Network Synthesis and Design*, John Wiley and sons, Inc., New York, 1976.

[22] S.A. Klugman, H.H Panjer and G.E. Willmot, *Loss Models: From Data to Decisions*, John Wiley and Sons, Inc., New York, 2008.

[23] W.W. Hines, D.C. Montgomery, D.M. Goldsman and C.M. Borror, *Probability and Statistics in Engineering*, John Wiley and Sons, Inc., New York, 2003.

[24] C. Forbes, M. Evans, N. Hastings and B. Peacock, *Statistical Distributions*, 4th ed., John Wiley and Sons, Inc., New York, 2011.

APPENDIX

Overview of Kolmogorov-Smirnof goodness of fit test

According to [22], the concept of the KolmogorovSmirnof goodness of fit test (KS-test) is to compare the KS-test statistic (KS) and the critical value (c) where it can be stated that the accuracy of each modelling result is satisfied if and only if $KS \leq c$ and the accuracy is inversely proportional to the KS. In the context of this work, KS can be mathematically defined with equations A1, A2 and, A3.

$$KS = \max_{\delta I_{Dj}/I_{Dj}} [|G_j(\frac{\delta I_{Dj}}{I_{Dj}})| - |F_j(\frac{\delta I_{Dj}}{I_{Dj}})|] \quad \text{(A1)}$$

$$F_j(\frac{\delta I_{Dj}}{I_{Dj}}) = \int_{-\infty}^{\delta I_{Dj}/I_{Dj}} f_j(x)dx \quad \text{(A2)}$$

$$G_j(\frac{\delta I_{Dj}}{I_{Dj}}) = \int_{-\infty}^{\delta I_{Dj}/I_{Dj}} g_j(x)dx \quad \text{(A3)}$$

Generally, c depends on the confidence level. For the 99% confidence level has been assumed in this work, c can be given by [22] equation A4.

$$c = \frac{1.63}{\sqrt{n}} \quad \text{(A4)}$$

n denotes the number of runs of the Monte-Carlo simulation. Since we choose $n = 3000$, $c = 0.0297596$ can be obtained.

Analytical determination of other statistical parameters and useful probabilities of drain current variations

By using $f_N(\delta I_{DN}/I_{DN})$ and $f_P(\delta I_{DP}/I_{DP})$, other interesting statistical parameters of $\delta I_{DN}/I_{DN}$ and $\delta I_{DP}/I_{DP}$ beside their averages and variances can be determined. Firstly, the median values of $\delta I_{DN}/I_{DN}$ and $\delta I_{DP}/I_{DP}$ can be obtained by solving equation A5.

$$\int_{-\infty}^{m_j} f_i(\frac{\delta I_{Dj}}{I_{Dj}})d\frac{\delta I_{Dj}}{I_{Dj}} = \frac{1}{2} \quad \text{(A5)}$$

As a result, we have $m_N = m_P = 0$.

Since $\overline{\frac{\Delta I_{DN}}{I_{DN}}} = \overline{\frac{\Delta I_{DP}}{I_{DP}}} = 0$ as mentioned above, the second moments of $\delta I_{DN}/I_{DN}$ and $\delta I_{DP}/I_{DP}$ can be mathematically defined with equation A6.

$$\overline{\left(\frac{\Delta I_{Dj}}{I_{Dj}}\right)^2} = \int_{-\infty}^{\infty} (\frac{\delta I_{Dj}}{I_{Dj}})^2 f_i(\frac{\delta I_{Dj}}{I_{Dj}})d\frac{\delta I_{Dj}}{I_{Dj}} \quad \text{(A6)}$$

As a result, we get equations A7 and A8.

$$\overline{\left(\frac{\Delta I_{DN}}{I_{DN}}\right)^2} = \frac{q^{1.5}\alpha^2\sqrt{2N_a(2\phi_F + V_S - V_B)\varepsilon_s}}{3WLC_{ox}C_{inv}(\sum_{i=1}^{N} k_iV_i + k_{fd}V_D + k_{fs}V_S + k_{fb}V_B - V_S - V_t)^2} \quad (29)$$

$$\overline{\left(\frac{\Delta I_{DP}}{I_{DP}}\right)^2} = \frac{q^{1.5}\alpha^2\sqrt{2N_a(2|\phi_F| - V_S + V_B)\varepsilon_s}}{3WLC_{ox}C_{inv}(\sum_{i=1}^{N} k_iV_i + k_{fd}V_D + k_{fs}V_S + k_{fb}V_B - V_S - V_t)^2} \quad (30)$$

Moreover, the moment generating functions of $\Delta I_{DN}/I_{DN}$ and $\Delta I_{DP}/I_{DP}$ can be defined as shown in equation A9.

$$M_j(t) = \int_{-\infty}^{\infty} \exp(\frac{\delta I_{Dj}}{I_{Dj}})^2 f_i(\frac{\delta I_{Dj}}{I_{Dj}})d\frac{\delta I_{Dj}}{I_{Dj}} \quad \text{(A9)}$$

Therefore we get equations A10 and A11.

$$M_N(t) = \exp\left[\frac{q^{1.5}\alpha^2\sqrt{2N_a(2\phi_F + V_S - V_B)\varepsilon_s}}{6WLC_{ox}C_{inv}(\sum_{i=1}^{N} k_iV_i + k_{fd}V_D + k_{fs}V_S + k_{fb}V_B - V_S - V_t)^2}\right] \quad (31)$$

$$M_p(t) = \exp\left[\frac{q^{1.5}\alpha^2\sqrt{2N_a(2|\phi_F| - V_S + V_B)\varepsilon_s}}{6WLC_{ox}C_{inv}(\sum_{i=1}^{N} k_iV_i + k_{fd}V_D + k_{fs}V_S + k_{fb}V_B - V_S - V_t)^2}\right] \quad (32)$$

Apart from these statistical parameters, many probabilities of those events related to $\delta I_{DN}/I_{DN}$ and $\delta I_{DP}/I_{DP}$ can be analytically determined by applying $f_N(\delta I_{DN}/I_{DN})$ and $f_P(\delta I_{DP}/I_{DP})$. This is because these probabilities can be given in terms of the cumulative distribution functions [23] and survival functions [24] of $\delta I_{DN}/I_{DN}$ and $\delta I_{DP}/I_{DP}$ which in turn can be determined by using $f_N(\delta I_{DN}/I_{DN})$ and $f_P(\delta I_{DP}/I_{DP})$. Similarly to those statistical parameters, these probabilities has also been found to be helpful to the variability aware design. The cumulative distribution functions of $\delta I_{DN}/I_{DN}$ and $\delta I_{DP}/I_{DP}$, $f_N(\delta I_{DN}/I_{DN})$ and $f_P(\delta I_{DP}/I_{DP})$, which have been mathematically defined by (A2) can be obtained after applying $f_N(\delta I_{DN}/I_{DN})$ and $f_P(\delta I_{DP}/I_{DP})$ as shown in equations A12 and A13.

$$F_N(\frac{\delta I_{DN}}{I_{DN}}) = \frac{1}{2}\left\{1 + erf\left[\frac{\sum_{i=1}^{N} k_iV_i + k_{fd}V_D + k_{fs}V_S + k_{fb}V_B - V_S - V_t}{\alpha(2N_a(2\phi_F + V_S - V_B)\varepsilon_s)^{0.25}}\sqrt{\frac{3WLC_{ox}C_{inv}}{2\pi q^{1.5}}(\frac{\delta I_{DN}}{I_{DN}})}\right]\right\} \quad (33)$$

$$F_P(\frac{\delta I_{DP}}{I_{DP}}) = \frac{1}{2}\left\{1 + erf\left[\frac{\sum_{i=1}^{N} k_iV_i + k_{fd}V_D + k_{fs}V_S + k_{fb}V_B - V_S - V_t}{\alpha(2N_a(2\phi_F + V_S - V_B)\varepsilon_s)^{0.25}}\sqrt{\frac{3WLC_{ox}C_{inv}}{2\pi q^{1.5}}(\frac{\delta I_{DP}}{I_{DP}})}\right]\right\} \quad (34)$$

$erf()$ denotes the error function which can be mathematically defined in terms of an arbitrary variable, y, as [23] does with equation A14.

$$erf(y) = \frac{2}{\sqrt{\pi}} \int_0^y \exp(-u^2)du \tag{A14}$$

On the other hand, the survival functions of $\delta I_{DN}/I_{DN}$ and $\delta I_{DP}/I_{DP}$ i.e. $S_N(\delta I_{DN}/I_{DN})$ and $S_P(\delta I_{DP}/I_{DP})$, which can be mathematically defined with equation A15.

$$S_j(\frac{\delta I_{Dj}}{I_{Dj}}) = \int\limits_{\delta I_{Dj}/I_{Dj}}^{\infty} f_j(x)dx \tag{A15}$$

j can be either N or P up to the type of the device under consideration, can be obtained by applying our $f_N(\delta I_{DN}/I_{DN})$ and $f_P(\delta I_{DP}/I_{DP})$ as shown in equations A16 and A17.

$$S_N(\frac{\delta I_{DN}}{I_{DN}}) = \frac{1}{2} - \frac{1}{2}erf\left[\frac{\sum\limits_{i=1}^{N} k_iV_i + k_{fd}V_D + k_{fs}V_S + k_{fb}V_B - V_S - V_t}{\alpha(2N_a(2\phi_F + V_S - V_B)\varepsilon_s)^{0.25}}\sqrt{\frac{3WLC_{ox}C_{inv}}{2\pi q^{1.5}}}(\frac{\delta I_{DN}}{I_{DN}})\right] \tag{35}$$

$$S_P(\frac{\delta I_{DP}}{I_{DP}}) = \frac{1}{2} - \frac{1}{2}erf\left[\frac{\sum\limits_{i=1}^{N} k_iV_i + k_{fd}V_D + k_{fs}V_S + k_{fb}V_B - V_S - V_t}{\alpha(2N_a(2\phi_F + V_S - V_B)\varepsilon_s)^{0.25}}\sqrt{\frac{3WLC_{ox}C_{inv}}{2\pi q^{1.5}}}(\frac{\delta I_{DP}}{I_{DP}})\right] \tag{36}$$

After obtaining $F_N(\delta I_{DN}/I_{DN})$, $F_P(\delta I_{DP}/I_{DP})$, $S_N(\delta I_{DN}/I_{DN})$ and $S_P(\delta I_{DP}/I_{DP})$, many probabilities of those interesting events related to $\delta I_{DN}/I_{DN}$ and $\delta I_{DP}/I_{DP}$ can be obtained as stated above. First, the probability that $\delta I_{DN}/I_{DN}$ lie within a certain predetermined range given by [a, b], and that of $\delta I_{DP}/I_{DP}$ i.e. $\Pr\{a \le \delta I_{DN}/I_{DN} \le b\}$ and $\Pr\{a \le \delta I_{DP}/I_{DP} \le b\}$, can be respectively obtained by using $F_N(\delta I_{DN}/I_{DN})$ and $F_P(\delta I_{DP}/I_{DP})$ as given by equations A18 and A19. This is because $F_j(x)$ is equivalent to the probability that $\delta I_{Dj}/I_{Dj} \le x$ where x can be arbitrary value of $\delta I_{Dj}/I_{Dj}$.

$$\Pr\{a \le \frac{\Delta I_{DN}}{I_{DN}} \le b\} = F_N(b) - F_N(a) \tag{A18}$$

$$\Pr\{a \le \frac{\Delta I_{DP}}{I_{DP}} \le b\} = F_P(b) - F_P(a) \tag{A19}$$

By using $\Pr\{a \le \Delta I_{DN}/I_{DN} \le b\}$ and $\Pr\{a \le \Delta I_{DP}/I_{DP} \le b\}$, the probability that the magnitudes of $\Delta I_{DN}/I_{DN}$does not exceed its allowable maximum value and the similar probability of $\Delta I_{DP}/I_{DP}$ i.e. $\Pr\{|\Delta I_{DN}/I_{DN}| \le |\Delta I_{DN}/I_{DN}|_{\max}\}$ and $\Pr\{|\Delta I_{DP}/I_{DP}| \le |\Delta I_{DP}/I_{DP}|_{\max}\}$, can be determined. This is because $|\Delta I_{Dj}/I_{Dj}| \le |\Delta I_{Dj}/I_{Dj}|_{\max}$ is equivalent to $-|\Delta I_{Dj}/I_{Dj}|_{\max} \le \Delta I_{Dj}/I_{Dj} \le |\Delta I_{Dj}/I_{Dj}|_{\max}$. So, we get equations A20 and A21.

$$\begin{aligned} &Pr\{\left|\frac{\Delta I_{DN}}{I_{DN}}\right| \le \left|\frac{\Delta I_{DN}}{I_{DN}}\right|_{\max}\} \\ &= Pr\{-\left|\frac{\Delta I_{DN}}{I_{DN}}\right|_{\max} \le \frac{\Delta I_{DN}}{I_{DN}} \le \left|\frac{\Delta I_{DN}}{I_{DN}}\right|_{\max}\} \\ &= F_N(\left|\frac{\Delta I_{DN}}{I_{DN}}\right|_{\max}) - F_N(-\left|\frac{\Delta I_{DN}}{I_{DN}}\right|_{\max}) \end{aligned} \tag{37}$$

$$\begin{aligned} &Pr\{\left|\frac{\Delta I_{DP}}{I_{DP}}\right| \le \left|\frac{\Delta I_{DP}}{I_{DP}}\right|_{\max}\} \\ &= Pr\{-\left|\frac{\Delta I_{DP}}{I_{DP}}\right|_{\max} \le \frac{\Delta I_{DP}}{I_{DP}} \le \left|\frac{\Delta I_{DP}}{I_{DP}}\right|_{\max}\} \\ &= F_P(\left|\frac{\Delta I_{DP}}{I_{DP}}\right|_{\max}) - F_P(-\left|\frac{\Delta I_{DP}}{I_{DP}}\right|_{\max}) \end{aligned} \tag{38}$$

In contrast to $\Pr\{a \le \Delta I_{DN}/I_{DN} \le b\}$ and $\Pr\{a \le \Delta I_{DP}/I_{DP} \le b\}$, the probability that $\Delta I_{DN}/I_{DN}$ lies outside $[a, b]$, and the similar one of $\Delta I_{DP}/I_{DP}$ which can be respectively denoted by $\Pr\{(\Delta I_{DN}/I_{DN} < a) \vee (\Delta I_{DN}/I_{DN} > b)\}$ and $\Pr\{(\Delta I_{DP}/I_{DP} < a) \vee (\Delta I_{DP}/I_{DP} > b)\}$ where $\vee$ stands for the or operator, can be obtained using $S_N(\delta I_{DN}/I_{DN})$ and $S_P(\delta I_{DP}/I_{DP})$ as given by equations A22 and (A23. This is because $S_j(x)$ is equivalent to the probability that $\Delta I_D/I_{Dj} > x$.

$$Pr\{(\frac{\Delta I_{DN}}{I_{DN}} < a) \vee (\frac{\Delta I_{DN}}{I_{DN}} > b)\} = 1 + S_N(b) - S_N(a) \tag{A22}$$

$$Pr\{(\frac{\Delta I_{DP}}{I_{DP}} < a) \vee (\frac{\Delta I_{DP}}{I_{DP}} > b)\} = 1 + S_P(b) - S_P(a) \tag{A23}$$

Similarly to obtaining $\Pr\{|\delta I_{DN}/I_{DN}| \le |\delta I_{DN}/I_{DN}|_{\max}\}$ and $\Pr\{|\delta I_{DP}/I_{DP}| \le |\delta I_{DP}/I_{DP}|_{\max}\}$ from $\Pr\{a \le \delta I_{DN}/I_{DN} \le b\}$ and $\Pr\{a \le \delta I_{DP}/I_{DP} \le b\}$, the probability that $|\delta I_{DN}/I_{DN}| > |\delta I_{DN}/I_{DN}|_{max}$ and that of $|\delta I_{DP}/I_{DP}| > |\delta I_{DP}/I_{DP}|_{\max}$ i.e., $\Pr\{|\delta I_{DN}/I_{DN}| > |\delta I_{DN}/I_{DN}|_{\max}\}$ and $\Pr\{|\delta I_{DP}/I_{DP}| > |\delta I_{DP}/I_{DP}|_{\max}\}$, can be respectively obtained by using $\Pr\{(\delta I_{DN}/I_{DN} < a) \vee (\delta I_{DN}/I_{DN} > b)\}$ and $\Pr\{(\delta I_{DP}/I_{DP} < a) \vee (\delta I_{DP}/I_{DP} > b)\}$. This is because $|(\delta I_{Dj}/I_{Dj}| > |(\delta I_{Dj}/I_{Dj}|_{\max}$ is equivalent to either having $\delta I_{Dj}/I_{Dj} < -|\delta I_{Dj}/I_{Dj}|_{\max}$ or $\delta I_{Dj}/I_{Dj} > |\delta I_{Dj}/I_{Dj}|_{\max}$. Therefore $\Pr\{|\delta I_{DN}/I_{DN}| > |\delta I_{DN}/I_{DN}|_{max}\}$ and $\Pr\{|\delta I_{DP}/I_{DP}| > |\delta I_{DP}/I_{DP}|_{max}\}$ can be respectively given by equations A24 and A25.

$$Pr\{\left|\frac{\Delta I_{DN}}{I_{DN}}\right| > \left|\frac{\Delta I_{DN}}{I_{DN}}\right|_{\max}\}$$
$$= Pr\{(\frac{\Delta I_{DN}}{I_{DN}} < -\left|\frac{\Delta I_{DN}}{I_{DN}}\right|) \vee (\frac{\Delta I_{DN}}{I_{DN}} > \left|\frac{\Delta I_{DN}}{I_{DN}}\right|_{\max})\} \quad (39)$$
$$= 1 + S_N(\left|\frac{\Delta I_{DN}}{I_{DN}}\right|_{\max}) - S_N(\left|\frac{\Delta I_{DN}}{I_{DN}}\right|_{\max})$$

$$Pr\{\left|\frac{\Delta I_{DP}}{I_{DP}}\right| > \left|\frac{\Delta I_{DP}}{I_{DP}}\right|_{\max}\}$$
$$= Pr\{(\frac{\Delta I_{DP}}{I_{DP}} < -\left|\frac{\Delta I_{DP}}{I_{DP}}\right|) \vee (\frac{\Delta I_{DP}}{I_{DP}} > \left|\frac{\Delta I_{DP}}{I_{DP}}\right|_{\max})\} \quad (40)$$
$$= 1 + S_N(\left|\frac{\Delta I_{DP}}{I_{DP}}\right|_{\max}) - S_N(\left|\frac{\Delta I_{DP}}{I_{DP}}\right|_{\max})$$

Apart from determining $\Pr\{|\delta I_{DN}/I_{DN}| > |\delta I_{DN}/I_{DN}|_{\max}\}$ and $\Pr\{|\delta I_{DP}/I_{DP}| > |\delta I_{DP}/ I_{DP}|_{\max}\}$, we can mathematically prove that the existence of ΔI_D of nanometer MIFGMOSFET of both types is absolutely certain by using $\Pr\{(\delta I_{DN}/I_{DN} < a) \vee (\delta I_{DN}/I_{DN} > b)\}$ and $\Pr\{(\delta I_{DP}/I_{DP} < a) \vee (\delta I_{DP}/I_{DP} > b)\}$. A similar prove for the above 100 nm device have been proposed in [14]. In the context of this research, it can be stated that the existence of ΔI_D is equivalent to having either $|\delta I_{DN}/I_{DN}| > 0$ or $|\delta I_{DP}/I_{DP}| > 0$ depending on the device type. Therefore the probability that ΔI_D occurs is equal to either $\Pr\{|\delta I_{DN}/I_{DN}| > 0\}$ or $\Pr\{|\delta I_{DP}/I_{DP}| > 0\}$. Since $|\delta I_{Dj}/I_{Dj}| > 0$ is equivalent to having either $\delta I_{Dj}/I_{Dj} < 0$ or $\delta I_{Dj}/I_{Dj} > 0$, we get equations A26 and A27.

$$Pr\{\left|\frac{\Delta I_{DN}}{I_{DN}}\right| > 0\} = Pr\{(\frac{\Delta I_{DN}}{I_{DN}} < 0) \vee (\frac{\Delta I_{DN}}{I_{DN}} > 0)\} \quad (A26)$$

$$Pr\{\left|\frac{\Delta I_{DP}}{I_{DP}}\right| > 0\} = Pr\{(\frac{\Delta I_{DP}}{I_{DP}} < 0) \vee (\frac{\Delta I_{DP}}{I_{DP}} > 0)\} \quad (A27)$$

By respectively applying equations A23 and A23 to equations A26 and A27, we have found that $\Pr\{\delta I_{DN}/I_{DN} > 0\} = 1$ and $\Pr\{\delta I_{DP}/I_{DP} > 0\} = 1$. This means that the probability that ΔI_D of the nanometer MIFGMOSFET of any type occurs is equal to 1. Therefore it can be stated that the existence of ΔI_D has been found to be absolutely certain for the nanometer MIFGMOSFET of both types. This emphasizes the unavoidability of ΔI_D and thus emphasizes the necessity of our work.

Apart from using $\Pr\{(\delta I_{DN}/I_{DN} < a) \vee (\delta I_{DN}/I_{DN} > b)\}$ and $\Pr\{(\delta I_{DP}/I_{DP} < a) \vee (\delta I_{DP}/I_{DP} > b)\}$, the certain existence of ΔI_D of nanometer MIFGMOSFET can also be mathematically proved in an alternative manner. According to [19], the probability that $\delta I_{DN}/I_{DN}$ is equal to x, which is an arbitrary fixed value, and the similar probability of $\delta I_{DP}/I_{DP}$, $\Pr\{\delta I_{DN}/I_{DN} = x\}$ and $\Pr\{\delta I_{DP}/I_{DP} = x\}$, can be given by equations A28 and A29.

$$Pr\{\frac{\Delta I_{DN}}{I_{DN}} = x\} = F_N(x) - F_N(x^-) \quad (A28)$$

$$Pr\{\frac{\Delta I_{DP}}{I_{DP}} = x\} = F_P(x) - F_P(x^-) \quad (A29)$$

x^- denotes the value of either $\delta I_{DN}/I_{DN}$ or $\delta I_{DP}/I_{DP}$ just before reaching x.

By such definition of x^-, we have found that $F_j(x)$ and $F_j(x^-)$ are almost equal. Therefore both $\Pr\{\delta I_{DN}/I_{DN} = x\}$ and $\Pr\{\delta I_{DP}/I_{DP} = x\}$are extremely low. Since x can be any value including 0, it can be seen that $\Pr\{\delta I_{DN}/I_{DN} = 0\}$ and $\Pr\{\delta I_{DP}/I_{DP} = 0\}$, which are equal to the probability of obtaining $\Delta I_D = 0$, are also extremely low. This means that the inexistence of ΔI_D is practically impossible, which implies that ΔI_D certainly exists.

As mentioned above, these probabilities have been found to be beneficial to the nanometer MIFGMOSFET involved variability aware design similarly to the statistical parameters. As an illustration, we consider $|\delta I_{Dj}/I_{Dj}| > |\delta I_{Dj}/I_{Dj}|_{\max}$, which means that ΔI_D exceeds the acceptably maximum level, as it is an undesirable event. For avoiding such event, the objective functions in equations A30 and A31 must be satisfied.

$$\min[Pr\{|\Delta I_{DN}/I_{DN}| > |\Delta I_{DN}/I_{DN}|_{\max}\}] \quad (A30)$$

$$\min[Pr\{|\Delta I_{DP}/I_{DP}| > |\Delta I_{DP}/I_{DP}|_{\max}\}] \quad (A31)$$

In addition, we often need ΔI_D to be within an acceptable limit that is we need $|\delta I_{Dj}/I_{Dj}| > |\delta I_{Dj}/I_{Dj}|_{\max}$. Therefore such a desired event will occur by satisfying the objective functions given in equations A32 and A33.

$$\max[Pr\{|\Delta I_{DN}/I_{DN}| > |\Delta I_{DN}/I_{DN}|_{\max}\}] \quad (A32)$$

$$\max[Pr\{|\Delta I_{DP}/I_{DP}| > |\Delta I_{DP}/I_{DP}|_{\max}\}] \quad (A33)$$

Similarly to the statistical parameter based objective functions, these probability based objective functions can be satisfied by tuning the controllable parameters mentioned previously as well.

Rawid Banchuin received the B.Eng. degree in electrical engineering from Mahidol University, Bangkok, Thailand in 2000, the degree of M.Eng. in computer engineering and Ph.D. in electrical and computer engineering from King Mongkut's University of Technology Thonburi, Bangkok, Thailand in 2003 and 2008 respectively. At the present, he is an assistant professor of the Graduated School of Information Technology and Faculty of Engineering, Siam University, Bangkok, Thailand. His research interests are computation and mathematics in electrical and electronic engineering especially the fractional order and memristive devices, circuits and systems.

Roungsan Chaisricharoen received B.Eng., M.Eng. and Ph.D. degrees from the department of computer engineering, King Mongkut's University of Technology Thonburi, Bangkok, Thailand. He is an assistant professor at the school of information technology, Mae Fah Luang University, Chiang Rai, Thailand. His research interests are computational intelligence, analog circuits and devices, wireless networks and optimization techniques. At the present, Asst. Prof. Dr. Roungsan Chaisricharoen is a member of ECTI board committee, public relations personal of ECTI.